Int. J. Mol. Sci. **2011**, *12*, 9354-9368; doi:10.3390/ijms12129354

OPEN ACCESS

International Journal of

Molecular Sciences

ISSN 1422-0067

www.mdpi.com/journal/ijms

Article

QSAR Study and Molecular Design of Open-Chain Enaminones as Anticonvulsant Agents

Juan C. Garro Martinez [1,*], Pablo R. Duchowicz [2], Mario R. Estrada [1], Graciela N. Zamarbide [1] and Eduardo A. Castro [2]

[1] Department of Chemistry, National University of San Luis, Chacabuco 917, San Luis 5700, Argentine; E-Mails: estrada@unsl.edu.ar (M.R.E.); gzama@unsl.edu.ar (G.N.Z.)

[2] INIFTA, (CCT-La Plata-CONICET), Diag. 113 y 64, C.C. 16, Suc.4, La Plata 1900, Argentine; E-Mails: pabloducho@gmail.com (P.R.D.); eacast@gmail.com (E.A.C.)

* Author to whom correspondence should be addressed; E-Mail: jcgarro@unsl.edu.ar; Tel./Fax: +54-2652-423789 ext. 122.

Received: 15 September 2011; in revised form: 7 November 2011 / Accepted: 24 November 2011 / Published: 14 December 2011

Abstract: Present work employs the QSAR formalism to predict the ED_{50} anticonvulsant activity of ringed-enaminones, in order to apply these relationships for the prediction of unknown open-chain compounds containing the same types of functional groups in their molecular structure. Two different modeling approaches are applied with the purpose of comparing the consistency of our results: (a) the search of molecular descriptors via multivariable linear regressions; and (b) the calculation of flexible descriptors with the CORAL (CORrelation And Logic) program. Among the results found, we propose some potent candidate open-chain enaminones having ED_{50} values lower than 10 mg·kg^{-1} for corresponding pharmacological studies. These compounds are classified as Class 1 and Class 2 according to the Anticonvulsant Selection Project.

Keywords: QSAR theory; anticonvulsant activity; open-chain enaminone; flexible descriptors

1. Introduction

Enaminones are a group of organic compounds carrying the conjugated system N–C=C–C=O [1]. The literature reports information about the chemistry of enaminones, their physicochemical properties and biological activities [2–10]. In spite of the interest in these compounds, only a limited number of theoretical works have been published on the prototype enaminone 2-propenal-3-amine based on the semiempirical molecular orbitals theory [11,12] and the quantum chemical study using *ab initio* method or the density functional theory [13–15].

Biologically active enaminones may be classified in two different types, according to the layout of the functional group [13–15]: (a) open-chain enaminones (OCEs), where the characteristic group is part of a chain (thus having the flexibility that enables different conformers); and (b) ringed enaminones (REs), where the characteristic group is part of a ring and the enaminone group is not flexible. In recent years, a group of REs has been reported as anticonvulsant. The mechanism of action of these biomolecules would be similar to many classic antiepileptics and second-generation drugs, while they act on ion channels by blocking the passage of ions through them [2–10]. Among the bioactive REs appears DM5 (methyl 4-(4-chlorophenylamino), 6-methyl,2-oxocyclohex-3-ene carboxylate), (Figure 1a) and ON2 (ethyl 6-methyl,4-(5-methylisoxazol-3-ylamino), 2-oxocyclohex-3-ene carboxylate), (Figure 1b) [6,7]. Another family of enaminones with biological activity is derived from benzylamine enaminones, (Figure 1c) [9]. These have anticonvulsant activity similar to DM5 (aniline enaminone derivate) and ON2 (isoxasol enaminone derivate).

Figure 1. (**a**) Aniline enaminone derivative DM5. (**b**) Isoxasol enaminone derivative ON2. (**c**) Benzylamine enaminone derivative.

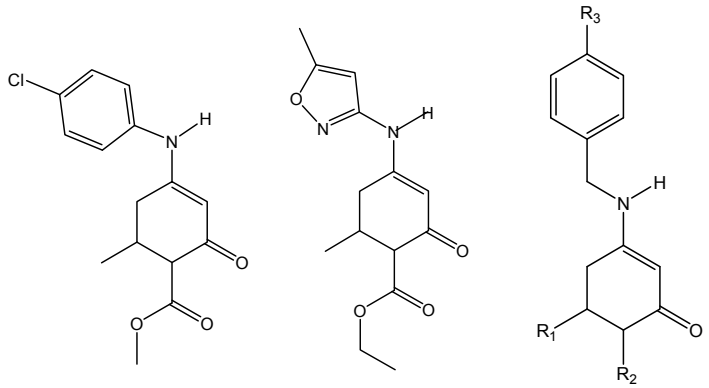

(**a**) (**b**) (**c**)

Distance between the carbonyl oxygen and the aromatic ring is of great importance during the binding of the molecule with the sodium channel [16]. Conformations that adopt a RE influence this distance may result in different activities [2–9]. In a previous study, we have performed a QSAR study on the activity of various RE in the active conformation [17].

Now, a comparison between both enaminone families demonstrates the similarity of the molecular structure and functional groups involved in the linkage with the sodium channel, as evidenced by the different pharmacophore models reported in the literature [16,18–20] (Figure 2). In this way, an OCE could bind to the receptor in a similar way as the REs do. Moreover for the OCE, the flexible open

chain and greater ability to transport through biological membranes would allow more precise fitting of its site of action.

Figure 2. Pharmacophore models reported in the literature and ringed and open-chain enaminones structures.

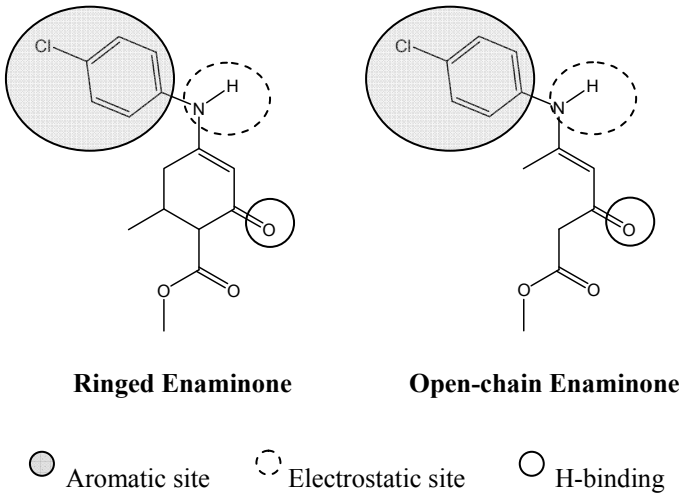

Accordingly, it is feasible to formulate the following question: could an open-chain enaminone have anticonvulsant activity as it is the case for ringed enaminones? Several techniques have been developed to elucidate a relationship between the structure and biological activity, SAR, QSAR [21], S-SAR [22–24]. The main objective of this work is to study a molecular set of OCEs for predicting their antiepileptic activity using the QSAR methodology, which would allow us to provide some guidelines on the anticonvulsant properties of this class of molecules.

2. Materials and Methods

2.1. Experimental Data

The experimental information on the antiepileptic activities of the molecular structures is obtained from various recent publications, by methods that have been previously reported [4–10]. Due to the scarcity of experimental information and the need for QSAR models, it is necessary to collect data from different authors [4–10]. However, we pay attention that the parameter of activity (ED_{50}), which represents the dose at which 50% of individuals reach the desired effect, is obtained by using the same assay. This is determined in the "Anticonvulsant Selection Project" (ASP) by the experimental method "Maximal electroshock seizure" (MES) [2,7,8,25]. For modeling purposes, we use Log_{10} ED_{50} to get a more standardized property.

2.2. Geometry Optimization and Molecular Descriptors Calculation

The structures of all the examined compounds are optimized with the Semiempirical Method PM3 (Parametric Method-3) included in the HyperChem 6.03 software [26]. By means of the software Dragon [27], we calculate a set of 1307 molecular descriptors [28], which includes. 0D: Constitutional Descriptors, 1D: Functional Groups, Empirics Descriptors, Atom Centred Fragments; 2D: Descriptors

topological, Molecular walk counts, Galvez Charge Index, BCUT Descriptors; 3D: Descriptors of Charge, aromatic index, molecular profiles of Randic, Geometry Descriptors, RDF Descriptors, 3D-Morse Descriptors, WHIM descriptors and GATEWAY Descriptors. In addition, 5 descriptors obtained from the semiempirical calculation are added (molecular dipole moment, energy of the HOMO and LUMO and HOMO-LUMO gap). Therefore, the set of descriptors contains $D = 1312$ variables.

2.3. Model Development

The QSAR established in this work are obtained via two different modeling approaches with the purpose of comparing the consistency of our results: (a) the search of molecular descriptors via multivariable linear regressions; and (b) the calculation of flexible descriptors with the CORAL (CORrelation And Logic) program.

2.3.1. Linear Descriptors Search

In the search for the best model we use the Matlab 7.0 [29]. Our quest is to find from the set of D descriptors a subset of d ones ($d <<< D$) with the minimum standard deviation (S), so we use the Replacement Method (RM) [30–32]. Standard deviation is defined as follows:

$$S = \frac{1}{(N-d-1)} \sum_{i=1}^{N} res_i^2 \quad (1)$$

where N is the number of molecules in the calibration set CC (molecular set used for calibration of the model), res_i is the residue of the molecule i (difference between experimental and predicted property of i).

The QSAR Theory searches for the best predictions of the activity, but it is a rule in practice that the models should be simple, interpretable, and have a descriptor per six or seven molecules in order to achieve satisfactory results [33]. Then, we calculate the maximum number of descriptors (d_{nm}) to be included in the linear regression equation as:

$$d_{\mathrm{nm}} = \frac{N}{7} \quad (2)$$

On the other hand, the Kubinyi function *FIT* [34,35] is used to get the optimum number of descriptors (d_{opt}) of each linear regression established. The *FIT* criterion is a very effective method for obtaining the optimal number of descriptors of a particular model [32–34].

2.3.2. Calculation of Flexible Descriptors

CHEMPREDICT/CORAL (CORrelation And Logic) version 1.4 [36] is a freeware for Windows. Each molecular structure must be represented by SMILES (Simplified Molecular Input Line Entry System) notation, calculated with ACD/ChemSketch software [37]. CORAL approach is based on the presence of certain SMILES attributes occurring in the molecule which can be associated to the activity of the molecule under evaluation [38–41]. As SMILES attributes are used the symbols representing the chemical elements, cycles, branching of molecular skeleton, charges, *etc.* More specific details on the CORAL algorithm can be found in the recent literature [38–41].

2.3.3. Model Validation

A next step of current analysis is to verify the validation (predictive capability) of the QSAR relationships established on a calibration set of chemical structures. These must be predictive and capable to adapt equally-well on new structures (test set) that do not participate during the training of the model. We choose the well-known leave-one-out (loo) and leave-more-out (l-%-o) cross-validation procedures, where % represents the percentage of molecules removed from the calibration set. For l-%-o, we generate 1,000,000 cases of random molecules removal, where % = 10 (five compounds). The standard deviations S_{test} and $S_{l\text{-}\%\text{-}o}$ are calculated in this step.

3. Results and Discussion

3.1. QSAR on Ringed-Enaminones

In a previous work we have developed a mathematical model for the prediction of ED_{50} in REs compounds [17]. This model contains five molecular descriptors and involves a calibration set of 46 compounds. For such model (Equation 3), validation is performed with a set of five molecules, leading to $S_{test} = 0.232$ and $R_{test} = 0.835$:

$$\begin{aligned}\log_{10} ED_{50} = &-3.3102\,(\pm 0.579) + 3.7124\,(\pm 0,737)\,BELe6 - 2.3384\,(\pm 0.387)\,BELp8 + \\ &0.1282\,(\pm 0.017)\,RDF025v + 0.66732\,(\pm 0.118)\,Mor15e + 33.683.\,(\pm 5.16)\,R4e +\end{aligned} \quad (3)$$

$$N = 46;\ p < 10^{-4};\ R_{cal} = 0.870;\ S_{cal} = 0.206;\ R_{test} = 0.835;\ S_{test} = 0.232;\ R_{loo} = 0{,}925;$$
$$S_{loo} = 0.198;\ R_{l\text{-}10\text{-}o} = 0.712;\ S_{l\text{-}10\text{-}o} = 0.319$$

In this study, we propose a new five-descriptor model (Equation 4). The calibration is established with 51 compounds, including all compounds belonging to Equation 3. Thus, Equation 4 contains more biochemical information and its predictive power may be higher. This last model is applied to the same calibration and test sets of Equation 3, leading to:

$$\begin{aligned}\log_{10} ED_{50} = &\ 2.247(\pm 0.867) - 0.024(\pm 0.005)G(O...Cl) + 0.0072(\pm 0.014)RDF025m - \\ &0.238(\pm 0.044)RDF115m + 35.631(\pm 4.793)R4e^{+} + 0.402(\pm 0.076)\Delta E_{Homo-Lumo}\end{aligned} \quad (4)$$

$$N = 51;\ p < 10^{-4};\ R_{cal} = 0.864;\ S_{cal} = 0.209;\ R_{test} = 0.947;\ S_{test} = 0.204;\ R_{loo} = 0.847;$$
$$S_{loo} = 0.228;\ R_{l\text{-}\%\text{-}o} = 0.746;\ S_{l\text{-}\%\text{-}o} = 0.343$$

In Equation 3, *BELe6* and *BELp8* are BCUT descriptors, *RDF025v* is a Radial Distribution Function descriptor, *Mor15e* is a 3D-MoRSE descriptor and $R4e^{+}$ is a 3D GATEWAY descriptor. The structural variables appearing in Equation 4 combine multidimensional aspects of the molecular structure and are classified as follows: Radial Distribution Function descriptors (*RDF025m* and *RDF115m*), Geometrical (*G(O..Cl)*), GATEWAY ($R4e^{+}$) and HOMO-LUMO energy gap (*Homo-Lumo*). A brief explanation of the descriptors participating in both equations is provided in Table 1.

Table 1. Symbols and description for molecular descriptors involved in QSAR.

Descriptor	Type	Details
BELe6	BCUT	Lowest eigenvalue *n*. 6 of Burden matrix/weighted by atomic Sanderson electronegativities
BELp8		Lowest eigenvalue *n*. 8 of Burden matrix/weighted by atomic polarizabilities
RDF025v	Radial Distribution Function	Radial Distribution Function—2.5/weighted by atomic van der Waals volumes
RDF025m		Radial Distribution Function—2.5/weighted by atomic masses
RDF115m		Radial Distribution Function—11.5/weighted by atomic masses
Mor15e	3D-MoRSE	3D-MoRSE—signal 15/weighted by atomic Sanderson electronegativities
$R4e^+$	GETAWAY	*R* maximal autocorrelation of lag 4/weighted by atomic Sanderson electronegativities
G(O..Cl)	Geometrical	Sum of geometrical distances between O..Cl
Homo-Lumo	Quantum Chemical	HOMO-LUMO energy gap

The highest intercorrelation coefficient for the five descriptors of Equation 3 is 0.733. This is because *BELe6* and *BELp8* descriptors belong to the same BCUT family. In general, QSAR models accept intercorrelations up to the value 0.98, but the orthogonalization process can be used to give better analysis when necessary [42,43]. Equation 4 has low intercorrelations between descriptors, the highest value is 0.561. Only descriptor $R4e^+$ (*R* maximal autocorrelation of lag 4/weighted by atomic Sanderson Electronegativities) simultaneously appears in both equations and has low intercorrelations to the remaining ones.

Table 2 lists the compounds of both models, together with the experimental and predicted ED_{50} values. Figure 3 shows the experimental and predicted Log_{10} ED_{50} plot for the calibration and validation sets. From this figure it can be noted that the two enaminones of the validation set, **47** and **51**, are very well predicted. Dispersion plots of the residuals for the calibration and test sets are provided in the supplementary material. Such figures reveal that the behavior of the residuals in terms of the predictions follows a random distribution, in accordance to the assumption involved in linear regression analysis. No molecule in the set exhibits a residual larger than the value of S.

Table 2. Experimental and predicted Log_{10} ED_{50} antiepileptic activity values of the compounds of calibration set and test set.

No.	Chemical name	ED_{50} (mg·Kg^{-1})	Exp.	Equation 3	Equation 4	Equation 5
1	Ethyl 6-methyl-4-(5-methylisoxazol-3-ylamino)-2-oxocyclohex-3-enecarboxylate	68.39 [4]	1.835	1.815	1.831	1.813
2	Methyl 4-(4-cyanophenylamino)-6-methyl-2-oxocyclohex-3-enecarboxylate	248.31 [4]	2.395	2.229	2.252	2.226
3	Methyl 4-(4-chlorophenylamino)-6-methyl-2-oxocyclohex-3-enecarboxylate	26.18 [4]	1.418	1.509	1.466	1.517

Table 2. *Cont.*

4	2-acetamido-*N*-benzylpropanamide	76.38 [5]	1.883	1.716	1.677	1.634
5	2-acetamido-*N*-(3-fluorobenzyl)propanamide	77.27 [5]	1.888	1.945	1.791	1.994
6	2-acetamido-*N*-(2-fluorobenzyl)-2-(furan-2-yl)acetamide	39.99 [5]	1.602	1.215	1.294	1.315
7	2-acetamido-*N*-(3-fluorobenzyl)-2-(furan-2-yl)acetamide	13.27 [5]	1.123	1.132	1.291	1.315
8	2-acetamido-*N*-(4-fluorobenzyl)-2-(furan-2-yl)acetamide	12.68 [5]	1.103	1.302	1.228	1.315
9	2-acetamido-*N*-(2,5-difluorobenzyl)-2-(furan-2-yl)acetamida	23.77 [5]	1.376	1.577	1.522	1.448
10	2-acetamido-*N*-(2,6-difluorobenzyl)-2-(furan-2-yl)acetamide	62.95 [5]	1.799	1.604	1.631	1.687
11	2-acetamido-*N*-benzylpent-4-enamide	33.57 [5]	1.526	1.653	1.605	1.533
12	2-acetamido-*N*-benzyl-2-(tetrahydrofuran-2-yl)acetamide	51.64 [5]	1.713	1.770	1.272	1.746
13	2-acetamido-*N*-benzyl-2-(furan-2-yl)acetamide	10.28 [5]	1.012	1.383	1.252	1.182
14	2-acetamido-*N*-benzyl-2-(5-methylfuran-2-yl)acetamide	19.19 [5]	1.283	1.450	1.200	1.282
15	2-acetamido-*N*-benzyl-2-(1H-pyrrol-2-yl)acetamide	16.07 [5]	1.206	1.486	1.299	1.315
16	2-acetamido-*N*-benzyl-2-(5-methyl-1H-pyrrol-2-yl)acetamide	36.48 [5]	1.562	1.530	1.376	1.415
17	2-acetamido-*N*-benzyl-2-(thiophen-2-yl)acetamide	44.77 [5]	1.651	1.388	1.628	1.593
18	2-acetamido-*N*-benzyl-2-(thiophen-3-yl)acetamida	87.70 [5]	1.943	1.783	1.770	1.979
19	2-acetamido-*N*-benzyl-2-(1H-pyrrol-1-yl)acetamide	80.17 [5]	1.904	1.572	1.538	1.399
20	2-acetamido-*N*-benzyl-2-(1H-pyrazol-1-yl)acetamide	16.48 [5]	1.217	1.249	1.294	1.325
21	2-acetamido-*N*-benzyl-2-(pyridin-2-yl)acetamide	10.79 [5]	1.033	0.880	1.037	1.195
22	2-acetamido-3-amino-*N*-benzyl-3-thioxopropanamide	86.50 [5]	1.937	1.550	1.921	1.981
23	2-acetamido-*N*-benzyl-2-(ethylamino)acetamide	42.36 [5]	1.627	1.525	1.635	1.679
24	2-acetamido-*N*-benzyl-2-(hydroxy(methyl)amino)acetamide	29.99 [5]	1.477	1.465	1.215	1.712
25	2-acetamido-*N*-benzyl-2-(1-phenylhydrazinyl)acetamide	42.76 [5]	1.631	1.524	1.663	1.811
26	2-acetamido-*N*-benzyl-2-ethoxyacetamide	61.94 [5]	1.792	1.795	1.922	1.368
27	2-acetamido-*N*-benzyl-3-methoxypropanamide	8.30 [5]	0.919	0.954	1.135	1.201
28	2-acetamido-*N*-benzyl-3-ethoxypropanamide	16.98 [5]	1.230	1.232	1.385	1.197
29	2-acetamido-*N*-benzyl-2-(pyrazin-2-yl)acetamide	14.79 [5]	1.170	0.929	1.015	0.893

Table 2. *Cont.*

30	2-acetamido-*N*-benzyl-2-(pyrimidin-2-yl)acetamida	8.09 [5]	0.908	1.151	1.344	1.121
31	2-acetamido-*N*-benzyl-2-(oxazol-5-yl)acetamide	10.50 [5]	1.021	0.998	1.149	0.88
32	2-acetamido-*N*-benzyl-2-(thiazol-5-yl)acetamide	11.99 [5]	1.079	1.417	1.717	1.291
33	2-acetamido-2-(3-aminophenylamino)-*N*-benzylacetamide	98.40 [5]	1.993	2.102	2.023	1.85
34	2-acetamido-*N*-benzyl-2-(furan-2-yl)acetamide	18.37 [5]	1.264	1.396	1.255	1.182
35	Ethyl 4-(4-chlorophenylamino)-6-methyl-2-oxo-3-cyclohexene-1-carboxylate	16.67 [7]	1.222	1.085	1.184	1.124
36	Ethyl 4-(4-bromophenylamino)-6-methyl-2-oxo-3-cyclohexene-1-carboxylate	7.89 [7]	0.897	1.259	0.861	1.383
37	Ethyl 6-methyl-2-oxo-4-(4-(trifluoromethoxy)phenylamino)cyclohex-3-enecarboxylate	37.07 [7]	1.569	1.708	1.831	1.553
38	Ethyl 4-(4-cianophenylamino)-6-methyl-2-oxo-3-cyclohexene-1-carboxylate	63.10 [7]	1.800	1.852	1.847	1.595
39	3-(4-chlorophenylamino)-5-methyl-2-cyclohexenone	40.36 [7]	1.606	1.804	1.570	1.576
40	3-(4-iodophenylamino)-5-methyl-2-cyclohexenone	76.91 [7]	1.886	1.924	1.829	1.835
41	Methyl 6-methyl-4-(5-methylisoxazol-3-ylamino)-2-oxocyclohex-3-cyclohexene-1-carboxylate	149.28 [8]	2.174	1.867	2.001	2.087
42	*Tert*-butyl 6-methyl-4-(5-methylisoxazol-3-ylamino)-2-oxocyclohex-3-cyclohexene-1-carboxylate	119.67 [8]	2.078	1.974	1.861	2.181
43	Methyl 4-(benzylamino)-6-methyl-2-oxocyclohex-3-cyclohexene-1-carboxylate	64.57 [9]	1.810	2.005	2.062	2.019
44	Methyl 4-(4-fluorobenzylamino)-6-methyl-2-oxocyclohex-3-cyclohexene-1-carboxylate	158.85 [9]	2.201	2.030	2.164	2.118
45	3-(benzylamino)-5,5-dimethylcyclohex-2-cyclohexenone	52.97 [9]	1.724	1.633	1.678	1.892
46	Methyl 4-(benzylamino)-6,6-dimethyl-2-oxocyclohex-3-enecarboxylate	131.83 [10]	2.120	2.219	2.107	1.904
47 *	Methyl 6-methyl-4-(4-nitrophenylamino)-2-oxocyclohex-3-enecarboxylate	299.92 [4]	2.477	2.441	2.793	2.599
48 *	2-acetamido-*N*-benzyl-2-phenylacetamide	20.28 [7]	1.307	1.505	1.347	1.269
49 *	2-acetamido-*N*-benzyl-2-(dimethylamino)acetamide	45.29 [7]	1.656	1.413	1.540	1.804
50 *	2-acetamido-2-(furan-2-yl)-*N*-(pyridin-3-ylmethyl)acetamide	29.99 [7]	1.477	1.396	1.255	1.182
51 *	5,5-dimethyl-3-(phenylamino)cyclohex-2-enone	109.14 [10]	2.038	1.812	1.990	1.434

* Molecules of test set.

Figure 3. Experimental and predicted Log_{10} ED_{50} plot. ○ Calibration set ● test set ▲ Enaminones of test set.

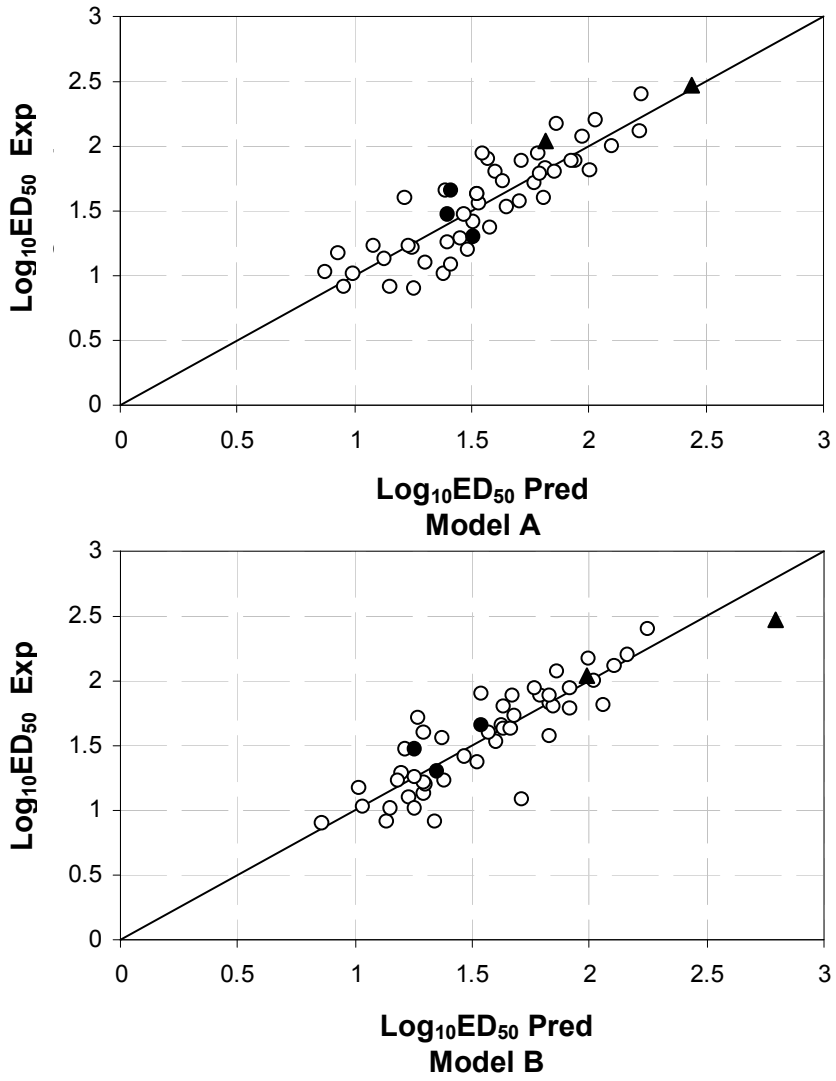

Now, it is feasible to improve the statistical performance of Equations 3 and 4 by using models established via flexible descriptor definitions calculated with the CORAL program. We run a Monte Carlo simulation for obtaining the DCW^3 descriptor of Equation 5, achieving the following QSAR model:

$$Log_{10}ED_{50} = -0.1906(\pm 0.0227) + 0.069(\pm 0.0008)DCW^3 \quad (5)$$

$$N = 46;\ p < 10^{-4};\ R_{cal} = 0.7627;\ S_{cal} = 0.192;\ R_{loo} = 0.6998;\ S_{loo} = 0.350$$

The specification of the numerical parameters used in the CORAL calculation is: number of epochs: 40, number of probes: 5, range of threshold values: 0–2, D_{start} = 0.1, $d_{precision}$ = 0.001, dR_{weight} = 0, dC_{weight} = 0, threshold range = 0–5, and $\alpha = \beta = 0$.

Figure 4 plots the predicted activities as function of the experimental data. The predictions achieved by model 5 are included in Table 2.

Figure 4. Experimental and predicted Log_{10} ED_{50} plot using flexible descriptors model: ○ Calibration set ● test set.

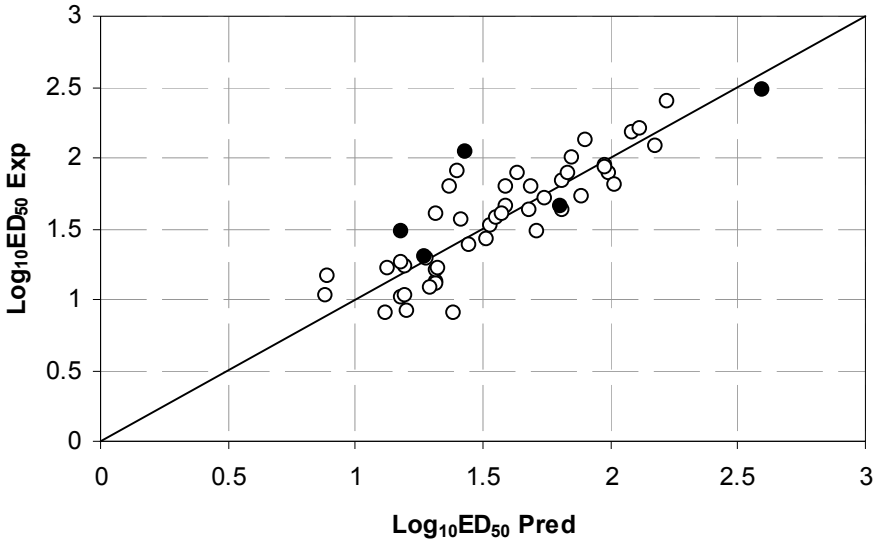

It is easily appreciated from the statistical parameters of calibration and leave-one-out validation that the quality of Equations 3 and 4 outperforms that of Equation 5. However, we decide to include Equation 5 in order to compare the predictions.

Another crucial problem to consider is the definition of the Applicability Domain (AD) of a QSAR model [44–46]. In other words, not even a robust, significant, and validated QSAR model can be expected to reliably predict the modeled property for the entire universe of molecules. In fact, only the predictions for molecules falling within this AD can be considered reliable and not just model extrapolations. The AD is a theoretical region in chemical space, and depends upon the set of chemical structures and the experimental property analyzed; hence the AD is different for each QSAR model established. We define the AD for each QSAR in terms of the ranges of variation of the numerical values of its descriptors: a molecular structure would be, in principle, reliably predicted if its numerical descriptor values fall within such ranges. Thus, for Equation (3) *BELe6*: [0.7180–1.0260], *BELp8*: [0.4540–1.0870], *RDF025v*: [12.2150–22.5420], *Mor15e*: [−0.6920–27.8150], $R4e^+$: [0.0330–0.0710]; for Equation (4) *G(O...Cl)*: [0.0000–32.1200], *RDF025m*: [13.9580–24.1070], *RDF115m*: [0.0000–4.8410], $R4e^+$: [0.0330–0.0710], $\Delta E_{Homo\text{-}Lumo}$: [−9.8192–(−7.8810)]; for Equation (5) DCW^3: [15.5091–40.4327]. In addition, the predicted activity for a considered structure based on a given combination of descriptors should fall inside (or close to) the range of the experimental activity variation, which in the present case is Log_{10} ED_{50}: [0.8970–2.4770].

3.2. QSAR on Open-Chain Enaminones

The selected OCEs are structurally-related to the REs used in the calibration and validation sets. For this selection, an analysis of molecular modulation is carried out, based on an active molecule. Then, the molecules **1A**, **1B**, **1C** and **1D** are obtained from molecules **3**, **51**, **43** and **41** (Figure 5). This figure shows the conformers of the OCEs. Molecules **3** and **51** belong to the family of aniline derivatives, **43** pertains to the family of benzylamine derivatives and **41** belongs to the family of isoxasol derivatives.

Figure 5. Structure of the 16 conformers of open-chain enaminones. Scheme for the selection of the compounds.

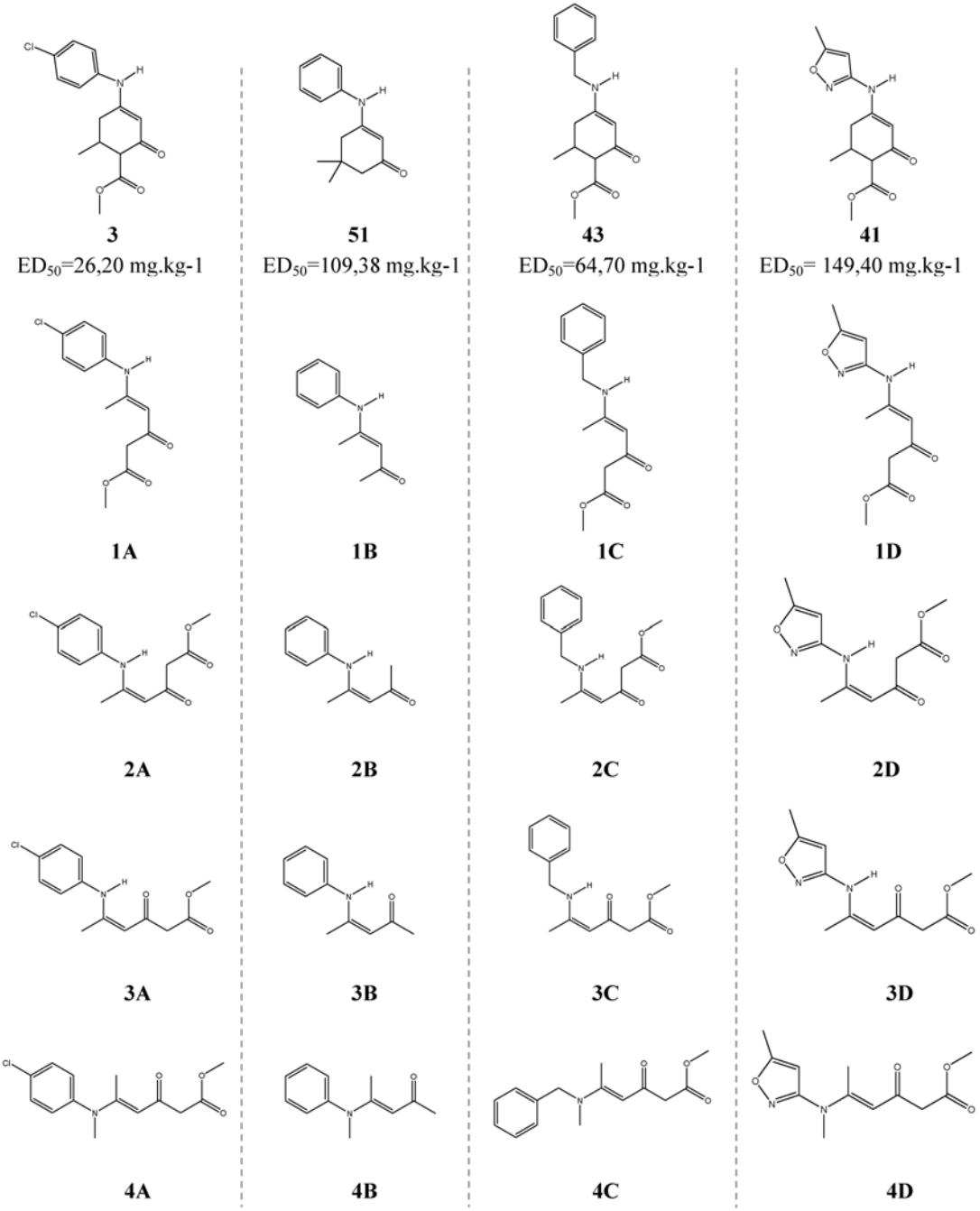

The structural similarity between the molecules used in the models and the OCEs suggests that the models developed in this work would serve to predict ED_{50} of these molecules. Having no experimental values, a way to verify the predictions is to note that Equations 3 and 4 do not lead to absurd predictions (different predictions for the same molecules). As shown in Table 3, the predictions are similar for both models. Both equations predict that **1B** is the most active, while the enaminone with lower activity is **3A**. Then, we argue that the predictions obtained are not at random, and that the predicted values of ED_{50} obtained with both models should be close to the experimental observations.

Table 3. Log_{10} ED_{50} for open-chain enaminones predicted by Equations 3 and 4.

Molecule	Equation 3	Equation 4	PSA [a]
1A	2.051	2.041	2
2A	2.426	2.093	2
3A	2.456	2.229	2
4A	2.323	2.037	2
1B	0.956	0.245	1
2B	1.529	0.903	1
3B	1.103	0.667	1
4B	1.393	0.758	1
1C	1.329	1.241	1
2C	1.462	1.556	1
3C	1.794	1.446	1
4C	1.505	1.177	1
1D	1.295	1.416	1
2D	1.583	1.375	1
3D	2.172	1.980	[b]
4D	1.291	1.183	1

[a] Anticonvulsant Screening Project (ASP) (21). Class 1: anticonvulsant activity at 100 $mg \cdot kg^{-1}$ or less; Class 2: anticonvulsant activity at doses greater than 100 $mg \cdot kg^{-1}$; Class 3: inactive at doses of 300 $mg \cdot kg^{-1}$. [b] Equation 4: Class 2; Equation 5: Class 1 (95 $mg \cdot kg^{-1}$).

4. Conclusions

A linear QSAR model is developed to predict ED_{50} in REs and applied for the prediction of OCEs. In addition, an alternative linear model using a different methodology based on the flexible descriptor definition is obtained with the same purpose. The developed models allow the prediction of antiepileptic activities of 16 OCEs. These compounds are presented as candidate structures for corresponding pharmacological studies. The 16 enaminones would be classified as Class 1 and Class 2 according to ASP. Several of the ED_{50} obtained here are less than 10 $mg \cdot kg^{-1}$. Accordingly, conformational flexibility in OCEs is a crucial factor to be considered during the study of the antiepileptic activity behaviour.

Acknowledgments

This work is supported by Consejo Nacional de Investigaciones Científicas y Técnicas (CONICET) project PIP11220100100151 and Universidad Nacional de San Luis (UNSL).

References

1. Cook, A.G. *Enaminas: Synthesis, Structure and Reaction*; Cook, A.G., Ed.; Marcel Dekker: New York, NY, USA, 1969.
2. Fraser, A.D. New drugs for the treatment of epilepsy. *Clin. Biochem*. **1996**, *29*, 97–110.
3. Porter, R.J.; Cereghino, J.J.; Gladding, G.D.; Hessie, B.J.; Kupferberg, H.J.; Scoville, B.; White, B.G. Antiepileptic drug development program. *Clevel. Clin. Q*. **1984**, *51*, 293–305.

4. Cox, D.S.; Gao, H.; Raje, S.; Scott, K.R.; Eddington, N.D. Enhancing the permeation of marker compounds and enaminone anticonvulsants across Caco-2 monolayers by modulating tight junctions using zonula occludens toxin. *Eur. J. Pharm. Biopharm*. **2001**, *52*, 145–150.
5. Cox, D.S.; Scott, K.R.; Gao, H.; Raje, S.; Eddington, N.D. Influence of multidrug resistance (MDR) proteins at the blood-brain barrier on the transport and brain distribution of enaminone anticonvulsants. *J. Pharm. Sci.* **2001**, *90*, 1540–1552.
6. Vamecq, J.; Lambert, D.; Poupaert, J.H.; Masereel, B.; Stables, J.P. Anticonvulsant activity and interactions with neuronal voltage-dependent sodium channel of analogues of ameltolide. *J. Med. Chem*. **1998**, *41*, 3307–3313.
7. Eddington, N.D.; Cox, D.S.; Khurana, M.; Salama, N.N.; Stables, J.P.; Harrison, S.J.; Negussie, A.; Taylor, R.S.; Tran, U.Q.; Moore, J.A.; *et al.* Synthesis and anticonvulsant activity of enaminones Part 7. Synthesis and anticonvulsant evaluation of ethyl 4-[(substituted phenyl)amino]-6-methyl-2-oxocyclohex-3-ene-1-carboxylates and their corresponding 5-methylcyclohex-2-enone derivatives. *Eur. J. Med. Chem*. **2003**, *38*, 49–64.
8. Eddington, N.D.; Cox, D.S.; Roberts, R.R.; Butcher, R.J.; Edafiogho, I.O.; Stables, J.P.; Cooke, N.; Goodwin, A.M.; Smith, C.A.; Scott, K.R. Synthesis and anticonvulsant activity of enaminones. 4. Investigations on isoxazole derivatives. *Eur. J. Med. Chem*. **2002**, *37*, 635–648.
9. Edafiogho, I.O.; Ananthalakshmi, K.V.; Kombian, S.B. Anticonvulsant evaluation and mechanism of action of benzylamino enaminones. *Bioorgan. Med. Chem*. **2006**, *14*, 5266–5272.
10. Kombian, S.B; Edafiogho, I.O.; Ananthalakshmi, K.V. Anticonvulsant enaminones depress excitatory synaptic transmission in the rat brain by enhancing extracellular GABA levels. *Br. J. Pharm*. **2005**, *145*, 945–953.
11. Eberlin, M.N.; Takahata Y.; Kascheres, C. The use of AM1 in structural analyses of primary and secondary enaminones. *J. Mol. Struct. (Theochem.)* **1990**, *207*, 143–156.
12. Kascheres, C.M. The chemistry of enaminones, diazocarbonyls and small rings: Our contribution. *J. Braz. Chem. Soc.* **2003**, *14*, 945–969.
13. Garro Martinez, J.C.; Manzanares, G.; Zamarbide, G.; Ponce, C.; Estrada M.; Jáuregui, E. Geometrical Isomerism, tautomerism and conformational charges of 2-propenal-3-amine in its neutral and protonated forms. *J. Mol. Struct. (Theochem.)* **2001**, *545*, 17–27.
14. Garro Martinez, J.C.; Zamarbide, G.N.; Ponce, C.; Estrada, M.R.; Tomás Vert F.; Ponce, C. Theoretical study of a hydration mechanism in an enaminone pro-drug prototype. *J. Mol. Struct. (Theochem.)* **2003**, *666–667*, 617–627.
15. Garro Martinez, J.C.; Zamarbide, G.N.; Estrada, M.R.; Castro, E.A. Geometrical isomerism and conformational charges of selected open-ring enaminones in its neutral and protonated forms. *J. Mol. Struct. (Theochem.)* **2005**, *725*, 63–68.
16. Carter, M.D.; Stephenson, V.C.; Weaver, D.F. Are anticonvulsants 'two thirds' of local anesthetics? A quantum pharmacology study. *J. Mol. Struct. (Theochem.)* **2003**, *638*, 57–62.
17. Garro Martinez, J.C.; Duchowicz, P.R.; Estrada, M.R.; Zamarbide G.N.; Castro, E. Anticonvulsant activity of ringed enaminones: A QSAR study. *QSAR Comb. Sci*. **2009**, *28*, 1376–1385.

18. Malawska, B.; Kulig, K.; Spiewak, A.; Stables, J.P. Investigation into new anticonvulsant derivatives of α-substituted *N*-benzylamides of γ-hydroxy- and γ-acetoxybutyric acid. Part 5: Search for new anticonvulsant compounds. *Bioorg. Med. Chem.* **2004**, *12*, 625–632.
19. Pandeya, S.N.; Raja, A.S. Synthesis of isatin semicarbazones as novel anticonvulsants—Role of hydrogen bonding. *J. Pharm. Sci.* **2002**, *5*, 266–271.
20. Aggarwal, N.; Mishra, P. Synthesis of 4-aryl substituted semicarbazones of some terpenes as novel anticonvulsants. *Pharm. Pharmaceut. Sci.* **2004**, *7*, 260–264.
21. Hansch, C.; Leo, A. *Exploring QSAR. Fundamentals and Applications in Chemistry and Biology*; American Chemical Society: Washington, DC, USA, 1995.
22. Lacrãmã, A.M.; Putz, V.M.; Ostafe, V. A spectral-SAR model for the anionic-cationic interaction in ionic liquids: Application to vibrio fischeri ecotoxicity. *Int. J. Mol. Sci*. **2007**, *8*, 842–863.
23. Putz, V.M.; Lacrãmã, A.M. Introducing spectral structure activity relationship (S-SAR) analysis. Application to ecotoxicology. *Int. J. Mol. Sci*. **2007**, *8*, 363–391.
24. Chicu, S.A.; Putz, M.V. Köln-timişoara molecular activity combined models toward interspecies toxicity assessment. *Int. J. Mol. Sci.* **2009**, *10*, 4474–4497.
25. National Institutes of Health. *Anticonvulsant Screening Project, Antiepileptic Drug Development Program*, DHEW Publication No. (NIH) 78-1093; NIH: Bethesda, MD, USA, 1978.
26. Hyperchem 7.5 (Hypercube). Available online: http://www.hyper.com/ (accessed on 22 July 2010).
27. Dragon 3.0 Evaluation Version. Available online: http://www.disat.unimib.it/chm (accessed on 6 November 2008).
28. Todeschini, R.; Consonni, V. *Handbook of Molecular Descriptors*; Wiley-VCH: Weinheim, Germany, 2000.
29. *Matlab 7.0*; The MathWorks Inc.: Natick, MA, USA, 2004.
30. Duchowicz, P.R.; Castro, E.A.; Fernández, F.M.; González, M.P. A new search algorithm for QSPR/QSAR theories. Normal boiling points of some organic molecules. *Chem. Phys. Lett.* **2005**, *412*, 376–380.
31. Duchowicz, P.R.; Castro, E.A.; Fernández, F.M. Alternative algorithm for the search of an optimal set of descriptors in QSAR-QSPR studies. *MATCH Commun. Math. Comput. Chem.* **2006**, *55*, 179–192.
32. Duchowicz, P.R.; Mercader, A.G.; Fernández, F.M.; Castro, E.A. Prediction of aqueous toxicity for heterogeneous phenol derivatives by QSAR. *Chemom. Intell. Lab. Syst.* **2008**, *90*, 97–107.
33. Andrea, T.A.; Kalayeh, H. Applications of neural networks in quantitative structure-activity relationships of dihydrofolate reductase inhibitors. *J. Med. Chem.* **1991**, *34*, 2824–2836.
34. Kubinyi, H. Variable selection in QSAR studies. II. A Highly efficient combination of systematic search and evolution. *Quant. Struct. Act. Relatsh.* **1994**, *13*, 393–401.
35. Kubinyi, H. Variable selection in QSAR studies. I. An evolutionary algorithm. *Quant. Struct. Act. Relatsh.* **1994**, *13*, 285–294.
36. Coral 1.4. Available online: http://www.insilico.eu/coral (accessed on 11 October 2010).
37. ACD/ChemSketch Freeware, version 12.01; Advanced Chemistry Development, Inc.: Toronto, ON, Canada, 2009. Available online: http://www.acdlabs.com (accessed on 11 November 2010).
38. Toropov, A.A.; Benfenati, E. SMILES in QSPR/QSAR Modeling: Results and perspectives. *Curr. Drug Discov. Technol.* **2007**, *4*, 77–116.

39. Toropov, A.A.; Benfenati, E. Additive SMILES-based optimal descriptors in QSAR modelling bee toxicity: Using rare SMILES attributes to define the applicability domain. *Bioorg. Med. Chem.* **2008**, *26*, 4801–4809.
40. Toropov, A.A.; Toropova, A.P.; Benfenati, E. Simplified molecular input line entry system-based optimal descriptors: Quantitative structure-activity relationship modeling mutagenicity of nitrated polycyclic aromatic hydrocarbons. *Chem. Biol. Drug Des.* **2009**, *73*, 515–525.
41. Toropov, A.A.; Toropova, A.P.; Benfenati, E.; Leszczynska, D.; Leszczynski, J. InChI-based optimal descriptors: QSAR analysis of fullerene [C60]-based HIV-1 PR inhibitors by correlation balance. *Eur. J. Med. Chem.* **2010**, *45*, 1387–1394.
42. Fernández, F.M.; Duchowicz, P.R.; Castro, E.A. Aplicación de los métodos QSAR/QSPR en fenómenos de adsorción de sustancias químicas sobre materiales sólidos. *MATCH Commun. Math. Comput. Chem.* **2004**, *51*, 39–57.
43. Fernández, F.M.; Castro E.A.; Duchowicz, P.R. Los descriptores ortogonales en la. Teoría QSAR-QSPR. *Afinidad* **2004**, *61*, 476–495.
44. Jaworska, J.; Nikolova-Jeliazkova, N.; Aldenberg, T. QSAR applicability domain estimation by projection of the training set in descriptor space: A review. *Altern. Lab. Anim.* **2005**, *33*, 445–459.
45. Gramatica, P. Principles of QSAR models validation: Internal and external. *QSAR Comb. Sci*. **2007**, *26*, 694–701.
46. Weaver, S.; Gleeson, M.P. The importance of the domain of applicability in QSAR modeling. *J. Mol. Graph. Model*. **2009**, *26*, 1315–1326.